Targeting of Porous Hybrid Silica Nanoparticles to Cancer Cells

Jessica M. Rosenholm,[†] Annika Meinander,[‡,§,⊥,¶] Emilia Peuhu,[‡,§,¶] Rasmus Niemi,[‡] John E. Eriksson,[‡,§] Cecilia Sahlgren,[‡,§,*] and Mika Lindén[†,*]

[†]Center for Functional Materials, Department of Physical Chemistry, Åbo Akademi University, Porthansgatan 3-5, FI-2500 Turku, Finland, [‡]Department of Biology, Åbo Akademi University, Artillerigatan 6A, FI-20520 Turku, [§]Turku Centre for Biotechnology, University of Turku and Åbo Akademi University, P.O. Box 123, FI-20521, Turku, Finland, and [⊥]Current address: The Breakthrough Toby Robins Breast Cancer Research Centre, Institute of Cancer Research, London SW3 6JB, United Kingdom. [¶]Both authors contributed equally to this work.

ABSTRACT Mesoporous silica nanoparticles functionalized by surface hyperbranching polymerization of poly(ethylene imine), PEI, were further modified by introducing both fluorescent and targeting moieties, with the aim of specifically targeting cancer cells. Owing to the high abundance of folate receptors in many cancer cells as compared to normal cells, folic acid was used as the targeting ligand. The internalization of the particles in cell lines expressing different levels of folate receptors was studied. Flow cytometry was used to quantify the mean number of nanoparticles internalized per cell. Five times more particles were internalized by cancer cells expressing folate receptors as compared to the normal cells expressing low levels of the receptor. Not only the number of nanoparticles internalized per cell, but also the fraction of cells that had internalized nanoparticles was higher. The total number of particles internalized by the cancer cells was, therefore, about an order of magnitude higher than the total number of particles internalized by normal cells, a difference high enough to be of significant biological importance. In addition, the biospecifically tagged hybrid PEI-silica particles were shown to be noncytotoxic and able to specifically target folate receptor-expressing cancer cells also under coculture conditions.

KEYWORDS: Cellular targeting · mesoporous silica · bioimaging · nanoparticles · surface functionalization

Targeting and drug delivery to specific cell populations are key aims in biomedical science today. Research efforts are, therefore, being placed on generating drug delivery systems to specifically target drugs to malfunctioning cells. Cellular targeting by utilizing antibodies or specific ligands rely on the capability of the targeting agents to selectively bind to the cell surface to trigger receptor-mediated endocytosis.[1] The drug delivery system along with the therapeutic agent would thereby be delivered to the interior of a given type of cells. Such a drug delivery system will not only have important therapeutic and pharmacological applications but also be of great interest for medical imaging and diagnosis. Targeting is especially relevant in the context of cancer therapies, as most of the commonly used anticancer drugs have serious side-effects due to unspecific action on healthy cells. The selectivity is a function of the ability of the nanoparticles to be internalized by the targeted cell population. But at least as important for the biological activity is the efficiency of uptake, that is, number of nanoparticles internalized by cancer cells in comparison to nontarget cells, as drug concentration is a key parameter for successful treatment.

The folate receptor, which normally is expressed only at the luminal surface of polarized epithelia, inaccessible to the circulation,[2,3] has been found to be overexpressed on the surface of several cancer cells, such as ovarian, endometrial, colorectal, breast, lung, renal cell carcinoma, brain metastases derived from epithelial cancer, and neuroendocrine carcinoma.[4,5] Because of this distinguishing feature between normal and cancer cells, folic acid, FA, has emerged as an attractive targeting ligand for selective delivery.[6] For a nanoparticulate delivery device, the challenge lies in successfully combining therapeutic and targeting actions with imaging capability into one system. In many cases, it is difficult to couple several functional groups in sufficient concentration, since the number of attachment sites on the particle surface is limited.[7] Moreover, each functionalization step might negatively affect the suspension stability of the particulate system, depending on the physicochemical properties of the added function.[7,8] Examples of drug delivery systems that have been successfully synthesized to combine targeting, imaging, and therapeutic moieties on their surface are dendrimers.[9−11] Dendrimers are nanometer sized, nonimmunogenic and hyperbranched "starburst polymers",[12] which because of the great number of terminal functional groups can be efficiently tailored for spatial distribution of biospecific moieties.[13] Furthermore, as these

*Address correspondence to Cecilia.Sahlgren@abo.fi, Mika.Linden@abo.fi.

Received for review September 26, 2008 and accepted December 05, 2008.

Published online December 23, 2008.
10.1021/nn800781r CCC: $40.75

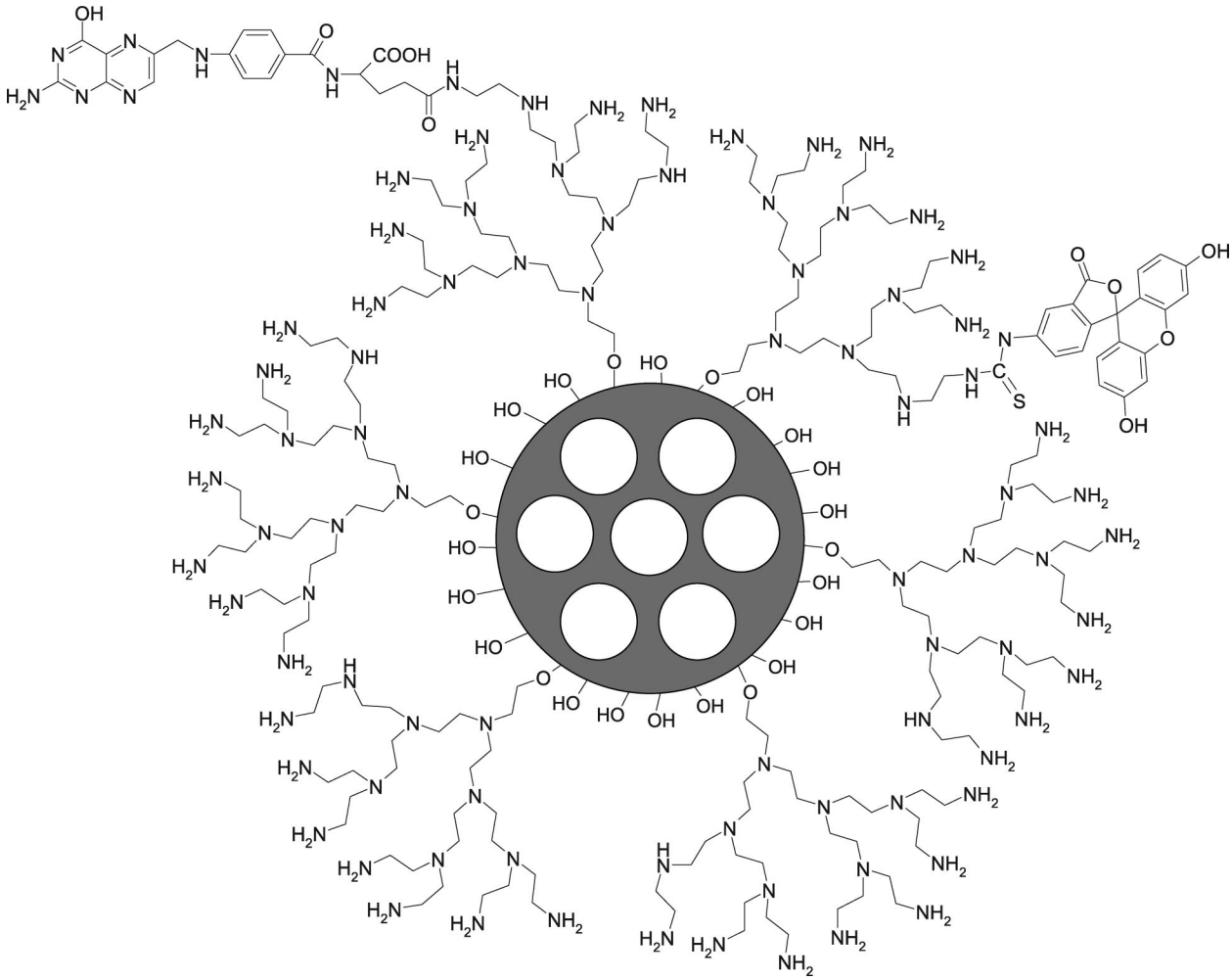

Figure 1. Schematic representation of the hybrid silica nanoparticle structure.

functional end groups are often primary amines, the high positive charge density provided by dendrimers and other polycations, such as poly(ethylene imine), PEI, are commonly applied as gene transfection agents. PEI has been reported to offer high gene delivery efficiency, since it exhibits a unique "proton-sponge"[14] or "endosome buffering" effect,[15] thus destabilizing lysosomal membranes and promoting endosomal escape. Because of these properties, recent interest has been focused toward the use of dendrimers as multifunctional FA-conjugated nanodevices for cancer therapy[7,9,10,16,17] and inflammatory tissue.[18]

Alongside with conventional polymeric carrier materials, ceramic structures have emerged as promising alternatives for drug delivery systems. Incorporation of drug substances into sol−gel derived silica (SiO_2) materials was introduced as early as 1983.[19] The sol−gel method is a simple and versatile low-temperature way of preparing porous, amorphous ceramic materials, which are stable toward light and heat, without being hazardous to humans or the environment.[20] Silica is an essential component of cells throughout the human body and amorphous silica is known to be nontoxic, biocompatible and biodegradable, being freely dispersible throughout the body and ultimately excreted in the urine. Especially room-temperature processed mesoporous silica is rapidly dissolved in water,[21] but when loaded with large amounts of guest molecules such as drugs, the aqueous solubility can be slowed down because of the increased hydrophobicity of the pore walls.[22] This large adsorption (drug loading) capacity is one of the many attractive features of mesoporous silica materials, accompanied by control of material properties on the nanometer scale such as pore and particle size. The drug content per mesoporous silica nanoparticle can be varied in a fairly straightforward fashion by optimizing the drug incorporation conditions.[22−24] The feasibility of mesoporous silica as a drug delivery system has, thus, been documented since the beginning of the millennium and has been subject to a number of reviews.[24−30] These studies have demonstrated examples of mesoporous silica as a vehicle for successful intracellular delivery of otherwise poorly soluble[31,32] or membrane-impermeable agents,[33] such as anticancer drugs. However, as was pointed out in a very recent review, cell type specificity is a challenge that still

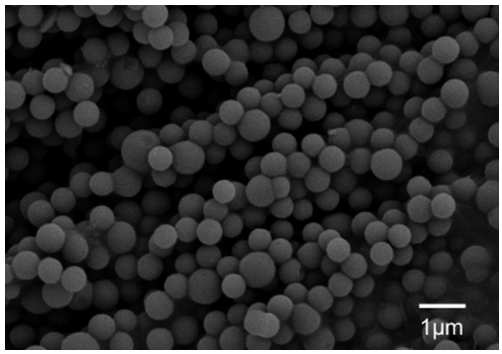

Figure 2. SEM image of APS-functionalized mesoporous silica nanoparticles.

needs to be overcome for these types of materials.[30]

Recently, we have reported the synthesis of hybrid PEI-mesoporous silica particles, where hyperbranched PEI is covalently linked to the silica surface by growing PEI *via* surface-polymerization.[34,35] Such hybrid particles are suggested to combine most of the positive features of dendrimers on the one hand, and mesoporous silica on the other, with regard to their use as drug carrier matrixes. While dendrimers are prepared by synthetic procedures involving iterative synthesis steps, hyperbranched polymers such as the PEI-function are conveniently prepared in one step. The ceramic carrier matrix furthermore effectively protects the payload molecules from (*e.g.*, enzymatic) degradation during delivery, as well as increases solubility and permeability of a drug with otherwise poor bioavailability.[36] The hybrid PEI-mesoporous silica particles have a much higher surface concentration of amino-groups as compared to corresponding materials prepared by classical co-condensation or postsynthesis grafting using aminosilanes.[35] As the isoelectric point, IEP, of the particles exceeds 9, their dispersion stability is dramatically enhanced as the surface maintains a high positive charge at physiological pH.[8] This is of great importance for the prevention of aggregation under physiological conditions. An additional level of flexibility of our approach is that the surface charge of the PEI-functionalized silica particles can be fine-tuned by chemical modifications such as succinylation,[37] to gain electrostatic stability under physiological pH conditions having a net negative outer surface charge on the particles. Importantly, the covalent attachment of the PEI layer to the particle surface ensures that the polymeric

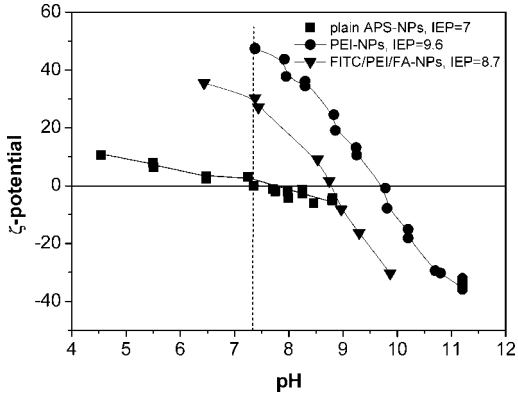

Figure 3. ζ -Potential titrations for mesoporous silica particles before (■) and after (●) PEI-functionalization, as well as after FITC- and FA-conjugation (▼). Dotted line at physiological pH indicates low electrostatic suspension stability for nonpolymer-modified particles.

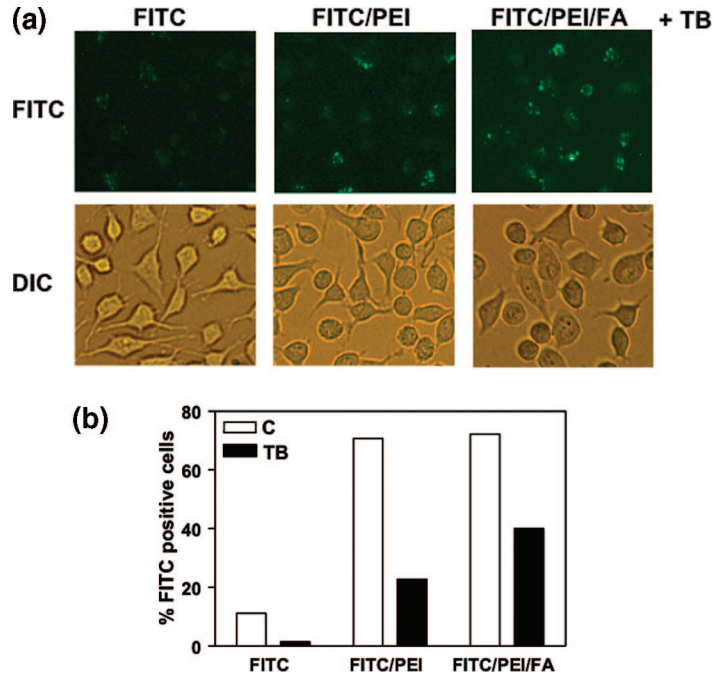

Figure 4. Folic acid-conjugation increases nanoparticle endocytosis in HeLa cells. HeLa cells were treated with nanoparticles at a dose of 10 μg/ml for 2 h and the extracellular binding of nanoparticles was quenched with trypan blue (FITC, pristine FITC-labeled particle; FITC/PEI, PEI-functionalized FITC-labeled particle; FITC/PEI/FA, folic acid-conjugated PEI-functionalized FITC-labeled particle). The FITC-labeled particles inside the cells were imaged by fluorescence microscopy and the cellular morphology by differential interference contrast (DIC) microscopy (A). The number of HeLa cells with endocytosed nanoparticles in control or trypan blue quenched cells was detected by flow cytometry (B). The results are representatives of at least three independent experiments.

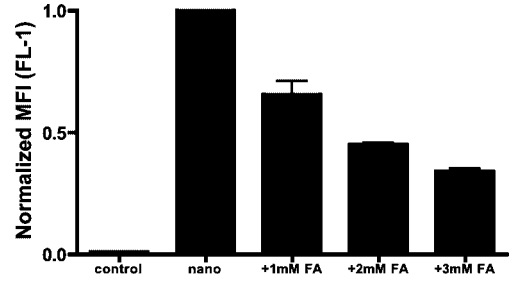

Figure 5. Folic acid competition inhibits specific particle endocytosis. HeLa cells were cultured overnight with 0−3 mM folic acid (FA) after which the cells were left untreated (control) or incubated with 10 μg/ml FITC/PEI/FA-functionalized nanoparticles (nano) for 4 h. After incubation the extracellular fluorescence was quenched by trypan blue and the endocytosed particles with FITC label were detected by flow cytometry. Mean fluorescence intensity (MFI) of FITC fluorescence in the cells was measured and the values normalized to particle endocytosis of HeLa cells (n = 2; mean ± SEM).

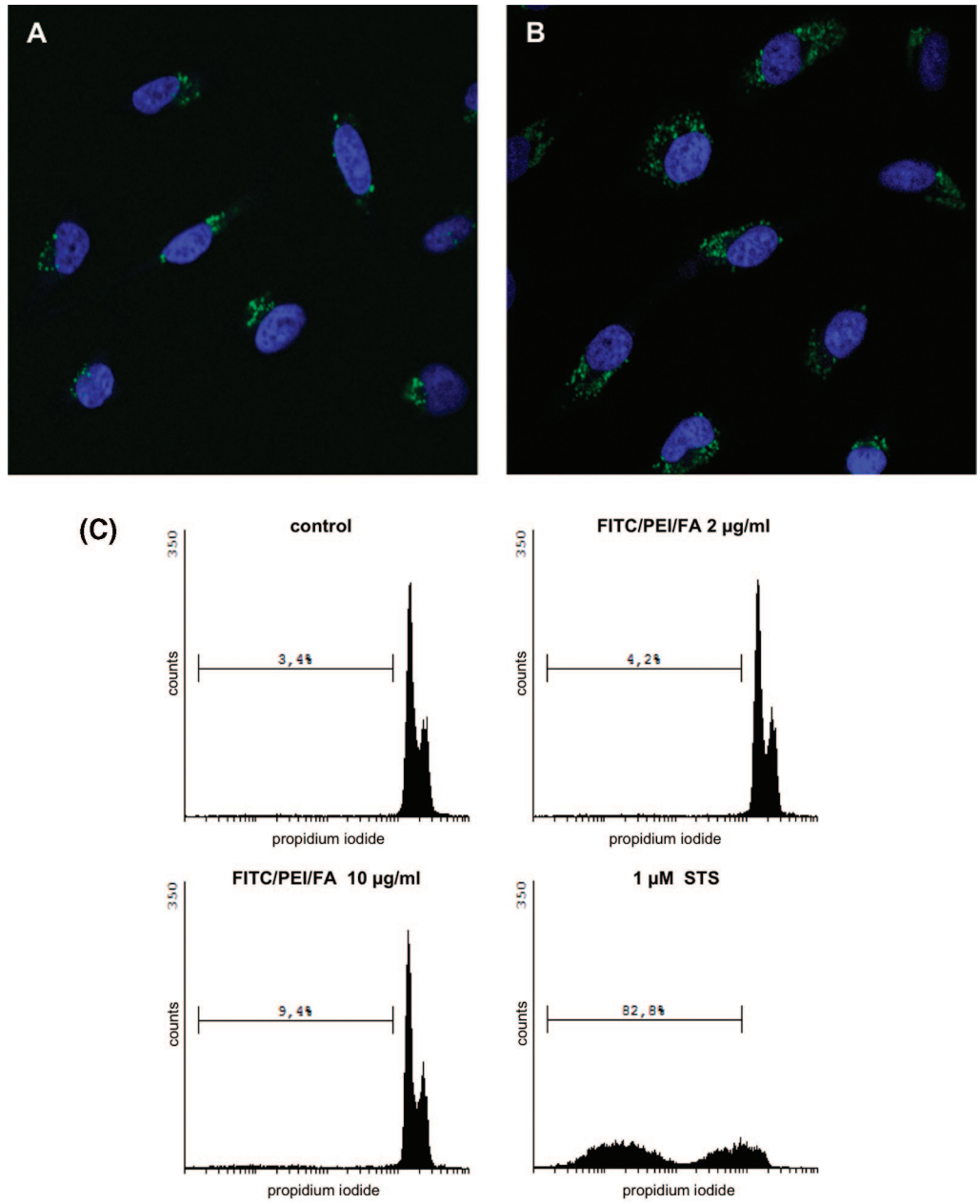

Figure 6. FITC/PEI/FA-functionalized silica nanoparticles do not induce cell death. HeLa cells were incubated with 2 μg/ml (A) or 10 μg/ml (B) of nanoparticles for 24 h. The endocytosed particles with FITC label (green) and DAPI-labeled cell nuclei (blue) were detected by confocal microscopy. Alternatively the cells were disrupted and the nuclei labeled for DNA content with propidium iodide. The samples were analyzed by flow cytometry and the fraction of sub-G0/G1 events was detected as a measure of apoptotic cell death (C). The relative fluorescence intensity of propidium iodide per cell was measured at the FL3-H channel. For a positive control the cells were treated with 1 μM staurosporine (STS). The results are representative of two independent experiments.

surface function remains on the particle throughout additional functionalization steps as well as during application. Our system thus carries similarities with a triple core−shell−shell architecture: an outer shell with one functionality such as targeting, an inner core consisting of a biodegradable mesoporous silica matrix able of carrying, protecting, and releasing large amounts of cargo; along with a middle PEI-layer which should enhance suspension stability, promote endosomal escape (see, for example, the recent study by Fuller *et al.*[38]) as well as provide reactive "hooks" that enable further modifications by standard bioconjugation routes.

To validate the applicability of our hybrid system in cancer cell-targeting applications, mesoporous nanoparticles with a mean diameter of about 400 nm were prepared and further functionalized with surface hyperbranching polymerization of PEI. This particle size was chosen since smaller particles typically show enhanced unspecific cellular uptake. For example, Lin *et al.* have shown that surface-functionalized 100 nm silica par-

ticles are effectively internalized by HeLa cells regardless of the surface composition of the particles.[39] Moreover, for amorphous silica, toxicity tends to be inversely related to particle size, and a particle size below 100 nm has actually been found to induce cytotoxicity in some cases.[40] A fluorescent dye, in the present case FITC, was covalently linked to the outer surface of the particles, making them visible by fluorescence microscopy and flow cytometry. Folic acid was used as the targeting ligand, and the cancer-specific internalization of these particles was tested on tumor and nontumor originating cells. HeLa cervical carcinoma cells were used as model cancer cells, as HeLa cells express the folate receptor-α (FR-α).[41] The embryonic kidney epithelial 293 cell line was used as a "folate receptor-negative" noncancerous cell model as the concentration of FR-α is much lower in these cells as compared to the HeLa cells. Importantly, the extracellular FITC was quenched with trypan blue (TB) in order to distinguish between the particles attached to the membrane and the particles internalized by the cells. Flow cytometry was used for the quantification of the fraction of cells that had internalized nanoparticles as the percent (%) of FITC positive cells among the given number of cells counted, as well as for measuring the mean quantity of nanoparticles internalized per cell as the mean fluorescence intensity among the counted cells. Even though investigations regarding cytotoxicity of mesoporous materials can be found in the literature (see for example refs 42−44), cytotoxicity seems to be particle-specific, and therefore cytotoxicity assays were also conducted. The endocytosis mechanism was verified by competing experiments with free folic acid, and the targetability was finally confirmed under coculture conditions.

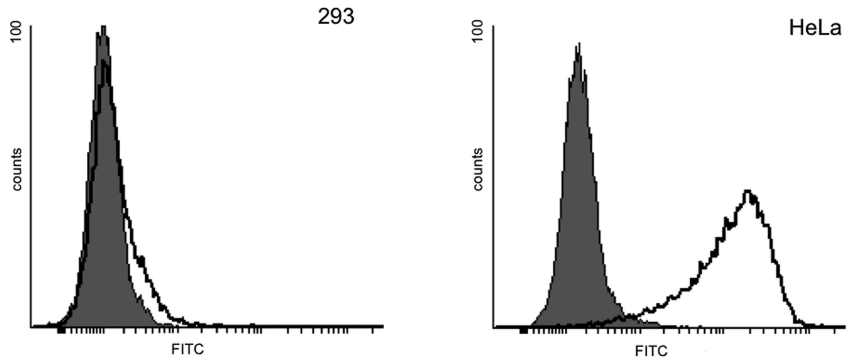

Figure 7. Folate receptor surface expression. HeLa cells and 293 cells were trypsinized and labeled with antifolate receptor primary antibody followed by Alexa488-conjugated secondary antibody (black line). Nonspecific fluorescence was measured using the secondary antibody only (shaded area). The samples were analyzed by flow cytometry by measuring the relative fluorescence intensity of FITC per cell at the FITC-A channel. The results are representative of two independent experiments.

RESULTS AND DISCUSSION

Nanoparticle characterization. The investigated nanoparticulate system is schematically shown in Figure 1, and an SEM image of the particles is shown in Figure 2. Partially aminofunctionalized mesoporous silica nanoparticles with a mean diameter of about 400 nm were first synthesized using a mixture of aminotrimethoxysilane (APS) and tetramethoxysilane (TMOS) as the silica precursors and cetyltrimethylammonium chloride (CTACl) as the structure directing agent. The particles had an ordered arrangement of mesopores, a specific surface area of 850 m^2/g, a pore diameter of about 3.5 nm, and a pore volume of 0.6 cm^3/g (see Supporting Information). The corresponding values after PEI-functionalization were 720 m^2/g, 2.8 nm, and 0.34 cm^3/g, respectively. The PEI content of the hybrid silica particles was 18 wt % as determined by thermogravimetry and the particle size distribution was measured by dynamic light scattering, indicating that no particle aggregation had occurred during functionalization (see Supporting Information). The particles were then fluorescently labeled by covalently attaching FITC containing the amine specific −N═C═S group to primary amine groups on the surface-grown PEI or aminopropyl-groups in the case of nonpolymer-functionalized particles. Finally, the targeting ligand, folic acid, FA, was covalently attached to amino groups through carbodiimide coupling. The surface modifications can easily be followed by ζ-potential measurements, which are sensitive mainly to the outer surface of the nanoparticles. As seen in Figure 3, the isoelectric point, IEP, of the silica nanoparticles increased from 7 for the starting particles, to 9.6 upon PEI- functionalization, reflecting the pronounced increase in the surface amino group density. The ζ-potential titration curve of the PEI-functionalized particles did not show any hysteresis, demonstrating the high chemical stability of the PEI-silica linkage. The IEP remained virtually constant upon FITC conjugation, but decreased slightly but significantly upon conjugation of the acidic FA to the FITC/PEI particles, from 9.5 to 8.7, as expected (see Figure 3). Thus, the changes in the IEP of the particles suggest that the surface conjugations of PEI, FITC, and FA to the mesoporous silica particles were successful. The ζ-potential value at physiological pH of 7.4 was +30 mV, which makes the particles fully dispersible in water, in agreement with our previous study.[8] Importantly, the ζ-potential value, and therefore also the dispersability, remained unchanged also at physiological pH in a HEPES buffer solution, which is typically used for buffering cell media.

Cellular Uptake As a Function of Particle Surface Modification. The uptakes of the plain (FITC), FITC/PEI- and FITC/PEI/FA-functionalized nanoparticles by HeLa cancer cells were studied by fluorescence microscopy and flow cytometry under *in vitro* conditions. The HeLa cells were

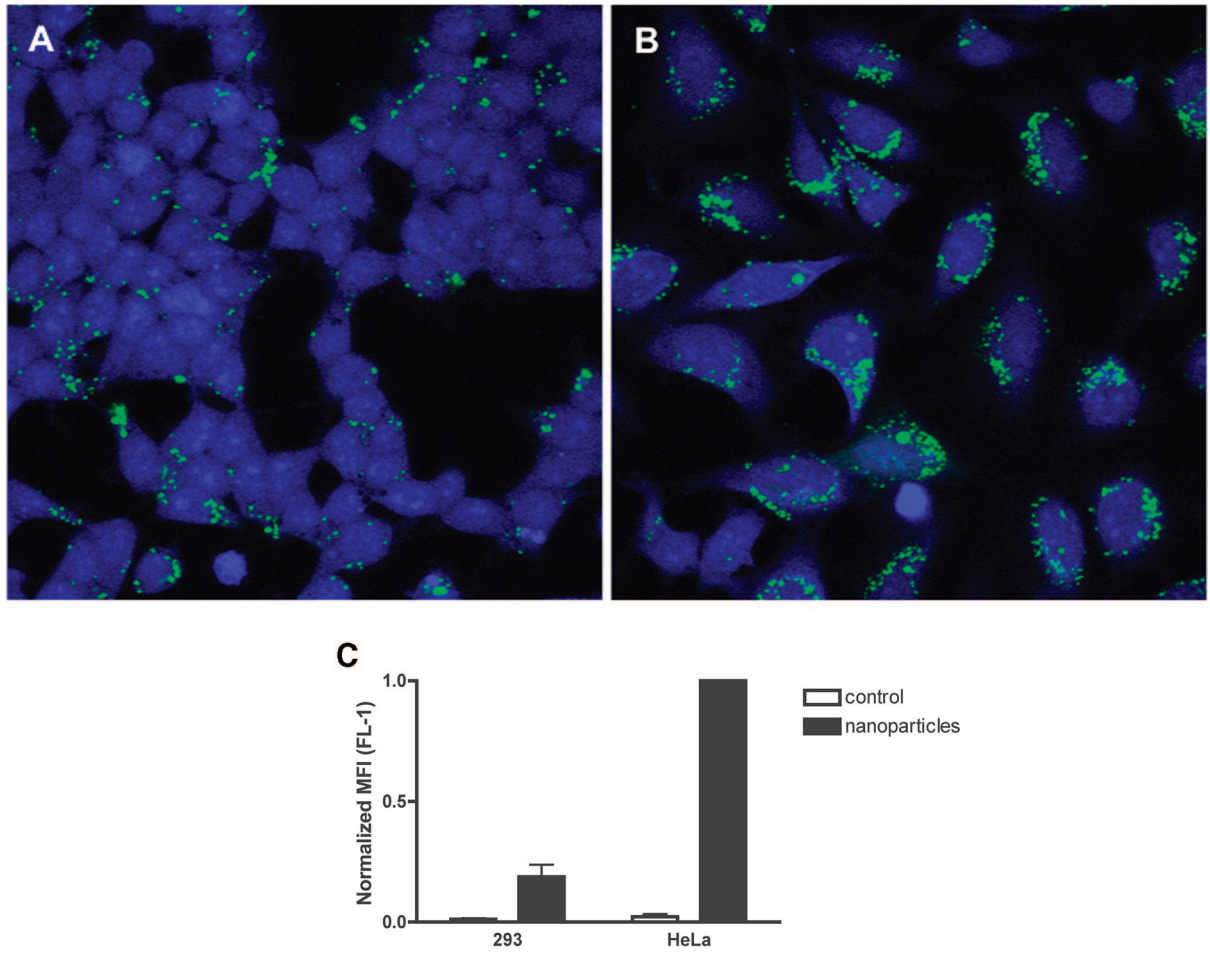

Figure 8. Specific particle endocytosis of FITC/PEI/FA-functionalized silica nanoparticles. 293 cells (A) or HeLa cells (B) were left untreated (control) or incubated with nanoparticles (10 μg/ml) for 4 h after which the extracellular fluorescence was quenched by trypan blue. The endocytosed particles with FITC label (green) inside CMAC-labeled (blue) cells were detected by confocal microscopy (A and B) or flow cytometry (C). Mean fluorescence intensity (MFI) of FITC in the cells was measured and the values were normalized to particle endocytosis in HeLa cells ($n = 3$; mean ± SEM).

incubated with nanoparticles for 2 h at 37 °C at a dose of 10 μg/ml. As shown in Figure 4B, flow cytometry measurements indicate that about 70% of the cells showed enhanced fluorescence when incubated with PEI-functionalized particles. As these particles carry a highly positive surface charge under the studied conditions, electrostatic attraction of the particles to the negatively charged cell membrane (−50 mV for HeLa cells) could account for this observation. To reliably distinguish between particles just attached to the outer part of the membrane and particles internalized by the cells, the extracellular FITC was quenched with trypan blue (TB). Interestingly, only about 20% of the FITC/PEI incubated cells showed remaining fluorescence in flow cytometry measurements after TB quenching, while the corresponding number was 40% for the FITC/PEI/FA incubated cells, as shown in Figure 4B. The level of fluorescence for the plain FITC-particles was equal to background fluorescence, indicating that virtually no particles were internalized in this case. This is opposite to the results obtained by Lin *et al.*, showing efficient uptake of FITC-labeled mesoporous nanoparticles at this concentration.[39] This difference can probably be ascribed to differences in particle size (100 nm particles were studied by Lin *et al.* as compared to about 400 nm particles in our case), as a smaller particle size may lead to enhanced nonspecific cellular uptake. For dye-functionalized mesoporous silica, a particle size of 50 nm has been reported to allow for the most efficient uptake in HeLa cells.[45]

Similar particle uptake was also detected after 24 h of incubation, as the fraction of FITC-positive cells was only 1.6% for the plain particles (FITC), whereas the corresponding values for FITC/PEI and FITC/PEI/FA were 24% and 52%, respectively (see Supporting Information). The data was recorded after TB quenching of extracellular fluorescence. Thus, virtually no uptake of plain FITC-particles by the HeLa cells was observed after 24 h. However, the HeLa cells showed enhanced fluorescence when exposed to nanoparticles functionalized with PEI, and much more so for the FITC/PEI/FA particles, indicating a successful discrimination between the biospecifically tagged and plain (FITC-labeled) particles,

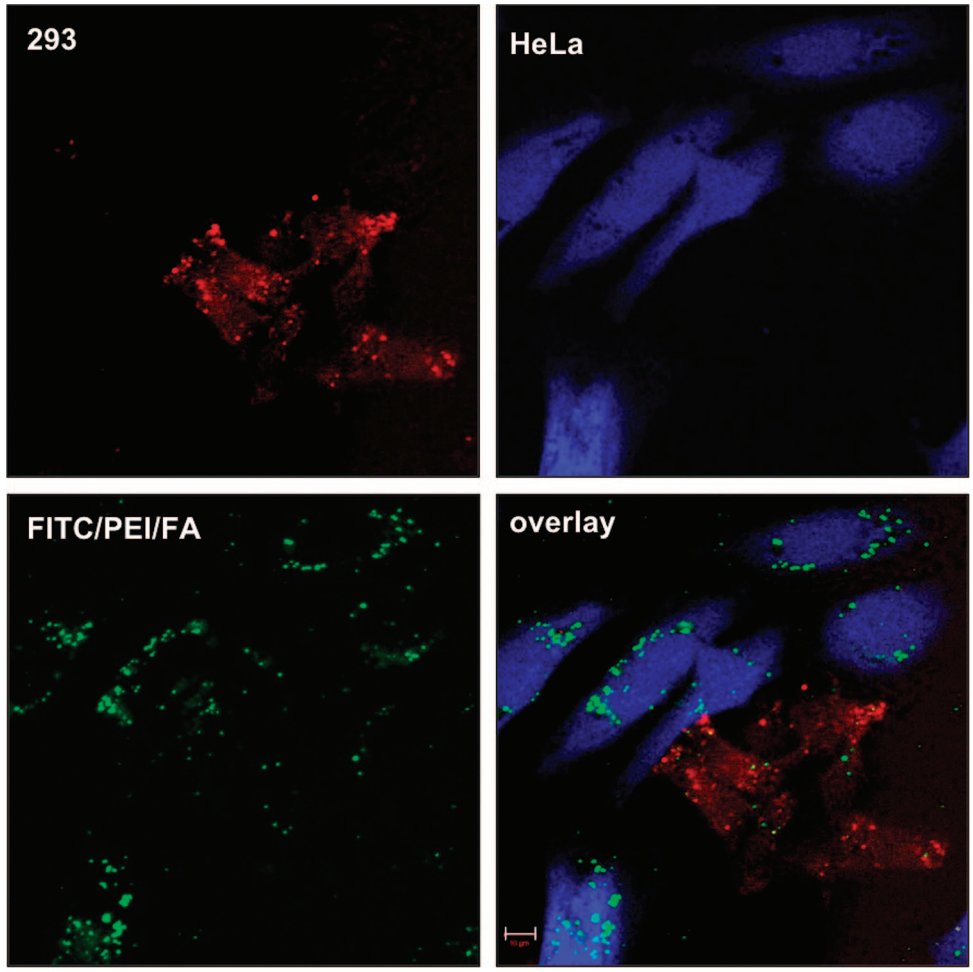

Figure 9. Specific endocytosis of FITC/PEI/FA-functionalized silica nanoparticles in coculture of HeLa and 293 cells. The cells were labeled with blue CMAC (HeLa) or CellTracker Red (293) and plated together overnight prior to incubation with the particles for 4 h. After incubation the extracellular fluorescence was quenched by trypan blue and the endocytosed particles with FITC-label (green) inside blue- or red-labeled cells were detected by confocal microscopy. Scale bar 10 μm. The results are representative of two independent experiments.

probably by recognition by the folate receptor followed by receptor-mediated endocytosis.

Folate-Receptor Mediated Uptake. To verify that the uptake is mediated *via* the folate receptor, a competition experiment using different amounts of free folic acid in the cell medium together with the FITC/PEI/FA -functionalized silica nanoparticles was performed. The number of HeLa cells that had internalized the FITC/PEI/FA-functionalized silica particles decreased with increasing concentration of free FA, as shown in Figure 5. At a free FA concentration of 3 mM the mean fluorescence intensity (MFI) value decreased to a value of about 1/3 of the value measured in the absence of free FA. The inhibition of uptake by free FA in a dose-dependent manner demonstrates that the particle uptake is mediated by the FA receptor. However, we note that as some internalization of nanoparticles occurs even at a concentration of free FA of 3 mM, some other cellular uptake mechanisms in addition to receptor-mediated endocytosis are operative, and our current efforts focus on minimizing the influence of nonspecific nanoparticle uptake by further optimization of the surface functionality of the particles.

Cellular Toxicity. To assess cellular toxicity of the particles, we determined the number of dying cells in cultures treated with high and low concentrations of FITC/PEI/FA nanoparticles for up to 24 h as compared to untreated cells. As the cellular uptake is fairly rapid and can be observed already after 2−3 h, toxicity would generally be observed within 24 h.[40,46] Nuclear morphology as determined by confocal microscopy of DAPI stained cells was used to assess the level of cell death (Figure 6AB). Cytotoxicity would be clearly evident by gross changes in nuclear morphology of cells undergoing apoptosis. The results show no difference in cell death over time in the treated *versus* untreated cells. This result was further quantified by a parallel experiment where we analyzed the nuclear morphology by flow cytometry of propidium iodide (PI)-stained nuclei (Figure 6C). The condition of the cells was furthermore monitored by light microscopy for up to 72 h after addition of the particles with no effects observed on cell

morphology (data not shown). Taken together, these results demonstrate that there are no signs of significant nanoparticle-induced cellular toxicity for a prolonged period of time.

Specific Internalization of FA-Conjugated Particles by Normal and Tumor Originating Cells. To positively identify the ability to target the FITC/PEI/FA-functionalized silica particles to HeLa cancer cells, we compared the nanoparticle uptake by HeLa and 293 cells under identical conditions. The embryonic kidney epithelial 293 cells express a much lower level of the folate receptor than the HeLa cells, as shown in Figure 7, although the 293 cells do express some folate receptors (Figure 7). A clearly higher number of the green fluorescent FITC/PEI/FA-functionalized silica particles are detected in the HeLa cells (Figure 8B), than in the 293 cells (Figure 8A). Flow cytometry measurements were performed to quantify the number of HeLa and 293 cells targeted by FITC/PEI/FA-functionalized silica particles. The number of HeLa cells that had internalized silica nanoparticles was consistently 2-fold, as compared to that of 293 cells (Supporting Information, Figure S6). Even more importantly, the mean fluorescence (MFI) values measured for the two cell types indicated that the FITC-positive HeLa cells had internalized 5−6 times more of the FITC/PEI/FA-functionalized silica nanoparticles, than had the 293 cells, as shown in Figure 8C. The total number of particles internalized by the HeLa cancer cells was therefore about an order of magnitude higher than the total number of particles internalized by 293 cells, a difference high enough to be of significant therapeutical importance. The selective uptake of FITC/PEI/FA particles by HeLa cells were additionally verified in coculture experiments, that is, where both HeLa cells and 293 cells were incubated together, as shown in Figure 9. The fact that green emission due to FITC was observed almost exclusively within HeLa cells confirms preferential uptake of the silica particles by the HeLa cancer cells with elevated folate receptor expression as compared to the noncancerous 293 cells, positively proving successful targeting of our hybrid silica particles also under coculture conditions.

CONCLUSIONS AND OUTLOOK

We have developed a selective nanoparticulate system for cancer cell targeting based on fluorescently labeled, PEI-functionalized and folic acid-conjugated mesoporous silica nanoparticles. The PEI function is grown by surface hyperbranching polymerization, and is thus covalently attached to the particle surface. This ensures full stability of the PEI-layer upon any further surface modifications and final application. Our results positively show that the PEI-mesoporous silica hybrid nanoparticles are nontoxic and furthermore can be specifically endocytosed using folic acid as the targeting ligand even under coculture conditions. The total number of particles internalized by the folate-receptor high cancer cells was about an order of magnitude higher than the total number of particles internalized by folate-receptor low normal cells, making the particles highly promising candidates for targeted drug delivery for cancer treatment or imaging agents for early tumor diagnosis.

The PEI surface layer can, if desired, easily be further modified for example by rational tuning of the particle surface charge,[37] as a complementary passive targeting strategy.[47] Furthermore, covalent linking of additional targeting ligands to the hyperbranched PEI layer is straightforward, which could lead to further increases in cell-type specificity, as tumor cells typically overexpress multiple types of surface receptors.[48] These aspects are currently under study in our laboratories.

METHODS

Preparation and Characterization of Mesoporous Silica Nanoparticles. Mesoporous silica nanoparticles were prepared according to a procedure described by Nakamura *et al.*,[49] with the difference that the thiol-silane was replaced by 3-aminopropyltrimethoxysilane, APS. In a typical synthesis, 1.19 g of tetramethoxysilane (TMOS) was mixed with APS under inert atmosphere and added to an alkaline solution containing the structure-directing agent cetyltrimethyl ammonium chloride (CTACl). The resulting synthesis mixture had a molar ratio of 0.9 TMOS: 0.1 APS: 1.27 CTACl: 0.26 NaOH: 1439 MeOH: 2560 H_2O. The sol was stirred overnight at room temperature(298 K), and thereafter aged for 8 h at static conditions. The precipitate was filtered off, washed with deionized water and dried at 318 K *in vacuo* for 72 h. The structure-directing agent was subsequently removed by ultrasonication in acidic (HCl) ethanol (about 0.12 w/w) three times.[50] The mesoscopic ordering of the nanoparticles was confirmed by powder-XRD using a Kratky compact small-angle system (M. Braun), particle size by dynamic light scattering (Malvern ZetaSizer Nano) and scanning electron microscopy (Jeol JSM-6335F, Jeol Ltd., Japan); and pore size, volume, and specific surface area by nitrogen sorption measurements (ASAP 2010 sorptometer, Micromeritics).

Poly(ethylene imine), PEI, was grown onto the mesoporous silica particles by hyperbranching surface polymerization according to procedures described in our earlier publications.[8,34,35,37] Thus, before poly(ethylene imine) functionalization, the surfactant-extracted particles were carefully vacuum-dried and subsequently subject to argon atmosphere. The particles (0.125 g) were immersed in toluene under inert atmosphere. Catalytic amounts of acetic acid and 45 μL of aziridine were added, and the reaction mixture was stirred overnight at 348 K. After the reaction, the particles were filtered off, washed with copious amounts of toluene, and vaccuum-dried for at least 24 h. The total amount PEI was calculated on the basis of thermogravimetric analysis (Netzsch TGA 209).

The particles, plain and PEI-functionalized, were labeled with FITC (fluorescein isothiocyanate) by suspending 25 mg of particles in carbonate buffer (pH 9), to which 250 μL of an ethanolic FITC-solution (1 mg/ml) was added and stirred for 30 min. After this, the PEI-functionalized particles were collected by centrifugation, washed with deionized water repeatedly, and subsequently suspended in MES buffer (pH 5). A 50 μg portion of folic acid was sonicated in MES, to which 20 μL of a 1 μL/ml EDC-solution (1-ethyl-3-(3-dimethylaminopropyl) carbodiimide) was added to activate the carboxylic acid groups of FA. This solution was rapidly added to the particle suspension, after which 25 μL

(1 mg/ml in MES) NHS (*N*-hydroxysuccinimide) solution was added to the suspension. The suspension was agitated overnight and washed with copious amounts of deionized water and ethanol, dried *in vacuo* and stored at 277 K.

Electrokinetic titrations were performed between each functionalization step using a Nano ZetaSizer setup (Malvern, Worcestershire, U.K.) coupled with an MPT-2 titrator unit. The ζ-potential was measured as a function of pH by titrating with 0.1 or 0.5 M HCl and NaOH at 298 K.

Cell Culture and Assessment of Particle Endocytosis. HeLa cervical carcinoma cells and HEK 293 (Human Embryonic Kidney) cells were cultured on 12-well plates in DMEM medium (Sigma) supplemented with 10% fetal calf serum (BioClear), 2 mM L-glutamin, 100 U/ml penicillin, 100 μg/ml streptomycin in 37 °C, 5% CO_2.

FITC-, FITC/PEI- or FITC/PEI/FA-functionalized silica nanoparticles were suspended in medium without antibiotics at a concentration of 10 μg/ml. After 30 min sonication in waterbath the medium containing the particles or control medium was applied to the 50−70% confluent cells and incubated for 2, 4, or 24 h at 37 °C. For folic acid competition experiments the cells were cultured overnight with 0−3 mM folic acid prior to addition of particles. The cells were trypsinized and the extracellular fluorescence was quenched by resuspension to 200 μg/ml trypan blue (Fluka) for 10 min at room temperature. The cells were washed once and resuspended in PBS. The amount of endocytosed particles inside cells was analyzed by LSRII or FacsCalibur flow cytometer (FITC-A or FL-I, BD Pharmingen). The mean fluorescence intensity (MFI) of the cells at FITC-A channel was measured. The data was analyzed with BD FacsDiva, and Cyflogic softwares. GraphPad Prism −software was used for the statistical analysis of the results. The bar graphs in the figures represent mean values (±SEM) from two or more independent experiments as indicated in the figure legends.

For microscopical studies the cells were labeled with 20 μM CMAC CellTracker (Invitrogen) or 5 μM CellTracker Red (Invitrogen) in medium without additives for 30 min and plated on glass-bottom culture dishes (MatTek Corp) in normal culture medium. After incubation with particles for 4 h, trypan blue was added to culture medium (200 μg/ml) and the cells were viewed live with Zeiss LSM 510 META laser-scanning confocal microscope (40× oil objective, 488 nm/405/545 nm excitation) or Leica DM Ibre inverted fluorescence microscope (16×, 20× objective).

Assessment of Cytotoxicity. For cytotoxicity analysis HeLa cells were plated on glass-bottom culture dishes (MatTek Corp) and incubated with 0, 2, or 10 μg/ml FITC/PEI/FA-functionalized nanoparticles for 24 h. Cell death was determined by analyzing changes in the nuclear morphology of DAPI-labeled cells with Zeiss LSM 510 META laser-scanning confocal microscope (40× oil objective, 488 nm/405 excitation). Alternatively the cells were collected by trypsinization and resuspended in propidium iodide (PI) buffer (40 mM Na-citrate, 0.3% Triton X-100, 50 μg/ml PI; Sigma). After 10 min incubation the samples were analyzed for nuclear fragmentation with FacsCalibur flow cytometer (FL-3, BD Pharmingen). The sub-G0/G1 peak was gated as a measure of nuclear fragmentation.

Folate Receptor Surface Expression. Surface expression of the Folate receptor was evaluated by indirect immunostaining using the anti-Folate receptor primary antibody (2 μg/ml, clone Mov18/ZEL, Alexis) followed by Alexa488 conjugated antimouse secondary antibody (Alexis Biochemicals). Nonspecific fluorescence was assessed using the secondary antibody only. Flow cytometric analyses were performed using an LSRII flow cytometer (FITC-A, BD Pharmingen).

Acknowledgment. M. Järn is thanked for performing the SEM-analysis and A. Duchanoy and B. Ufer are thanked for supplying the schematic image. The partial financial support from the Tor, Joe and Pentti Borg foundation as well as the financial support from the EU project NanoEar (contract number NMP4-CT-2006-026556) (J.M.R.) is gratefully acknowledged.

Supporting Information Available: Powder XRD pattern and nitrogen sorption isotherms for the studied material, as well as dynamic light scattering and thermogravimetry measurements. Flow cytometry measurements of the fraction of HeLa cells that has internalized differently functionalized nanoparticles after 24 h, as well as the fraction of HeLa as compared to 293 cells with internalized FITC/PEI/FA-functionalized nanoparticles. This material is available free of charge *via* the Internet at http://pubs.acs.org.

REFERENCES AND NOTES

1. Brandon-Peppas, L.; Blanchette, J. O. Nanoparticle and Targeted Systems for Cancer Therapy. *Adv. Drug Delivery Rev.* **2004**, *56*, 1649–1659.
2. Leamon, C. P.; Low, P. S. Folate-Mediated Targeting: From Diagnostics to Drug and Gene Delivery. *Drug Delivery Today* **2001**, *6*, 44–51.
3. Leamon, C. P.; Reddy, J. A. Folate-Targeted Chemotherapy. *Adv. Drug Delivery Rev.* **2004**, *56*, 1127–1141.
4. Elnakat, H.; Ratman, M. Distribution, Functionality and Gene Regulation of Folate Receptor Isoforms: Implications in Targeted Therapy. *Adv. Drug Delivery Rev.* **2004**, *56*, 1067–1084.
5. Sudimack, J.; Lee, R. J. Targeted Drug Delivery *via* the Folate Receptor. *Adv. Drug Delivery Rev.* **2000**, *41*, 147–162.
6. Low, P. S.; Henne, W. A.; Doorneweerd, D. D. Discovery and Development of Folic-Acid-Based Reptor Targeting for Imaging and Therapy of Cancer and Inflammatory Diseases. *Acc. Chem. Res.* **2008**, *41*, 120–129.
7. Harris, T. J.; von Malzahn, G.; Bhatia, S. N. Multifunctional Nanoparticles for Cancer Therapy. In *Nanotechnology for Cancer Therapy*; Amiji, M. M., Ed.; CRC Press: Boca Raton, FL, 2007; pp 59−76.
8. Bergman, L.; Rosenholm, J. M.; Öst, A.-B.; Duchanoy, A.; Kankaanpää, P.; Heino, J.; Lindén, M. On the Complexity of Electrostatic Suspension Stabilization of Functionalized Silica Nanoparticles for Biotargeting and -Imaging Applications. *J. Nanomater.* **2008**, doi:10.1155/2008/712514.
9. Majoros, I. J.; Thomas, T. P.; Mehta, C. B.; Baker, J. R., Jr. Poly(amidoamine) Dendrimer-Based Multifunctional Engineered Nanodevice for Cancer Therapy. *J. Med. Chem.* **2005**, *48*, 5892–5899.
10. Majoros, I. J.; Myc, A.; Thomas, T.; Mehta, C. B.; Baker, J. R., Jr. PAMAM Dendrimer-Based Multifunctional Conjugate for Cancer Therapy: Synthesis, Characterization, and Functionality. *Biomacromolecules* **2006**, *7*, 572–579.
11. Sideratou, Z.; Tziveleka, L. A.; Kontoyianni, C.; Tsiourvas, D.; Paleos, C. M. Design of Functionalized Dendritic Polymers for Application as Drug and Gene Delivery Systems. *Gene Ther. Mol. Biol.* **2006**, *10*, 71–94.
12. Tomalia, D. A.; Baker, H.; Dewald, J.; Hall, M.; Kallos, G.; Martin, S.; Roeck, J.; Ryder, J.; Smith, P. A New Class of Polymers: Starburst-Dendritic Macromolecules. *Polym. J.* **1985**, *17*, 117–132.
13. Agarwal, A.; Saraf, S.; Asthana, A.; Gupta, U.; Gajbhiye, V.; Jain, N. K. Ligand Based Dendritic Systems for Tumor Targeting. *Int. J. Pharmaceut.* **2008**, *350*, 3–13.
14. Godbey, W. T.; Wu, K. K.; Mikos, A. G. Poly(Ethylene Imine) and Its Role in Gene Delivery. *J. Controlled Release* **1999**, *60*, 149–160.
15. Lim, Y. B.; Kim, S. M.; Lee, Y.; Lee, W. K.; Yang, T.-G.; Lee, M.-J.; Suh, H.; Park, J.-S. Cationic Hyperbranched Poly(amino ester): A Novel Class of DNA Condensing Molecule with Cationic Surface, Biodegradable Three-Dimensional Structure, and Tertiary Amine Groups in the Interior. *J. Am. Chem. Soc.* **2001**, *123*, 2460–2461.
16. Quintana, A.; Raczka, E.; Piehler, L.; Lee, I.; Myc, A.; Majoros, I.; Patri, A. K.; Thomas, T.; Mulé, J.; Baker, J. R., Jr. Design and Function of a Dendrimer-Based Therapeutic Nanodevice Targeted to Tumor Cells Through the Folate Receptor. *Pharm. Res.* **2002**, *19*, 1310–1316.
17. Kukowska-Latallo, J. F.; Candido, K. A.; Cao, Z.; Nigavekar, S. S.; Majoros, I. J.; Thomas, T. P.; Balogh, L. P.; Khan, M. K.;

Baker, J. R., Jr. Nanoparticle Targeting of Anticancer Drug Improves Therapeutic Response in Animal Model of Human Epithelial Cancer. *Cancer Res.* **2005**, *65*, 5317–5324.
18. Chandrasekar, D.; Sistla, R.; Ahmad, F. J.; Khar, R. K.; Diwan, P. V. The Development of Folate-PAMAM Dendrimer Conjugates for Targeted Delivery of Anti-Arthritic Drugs and Their Pharmacokinetics and Biodistribution in Arthritic Rats. *Biomaterials* **2007**, *28*, 504–512.
19. Unger, K.; Rupprecht, H.; Valentin, B.; Kircher, W. The Use of Porous and Surface Modified Silicas as Drug Delivery and Stabilizing Agents. *Drug Deliv. Ind. Pharm.* **1983**, *9*, 69–91.
20. Böttcher, H.; Slowik, P.; Süss, W. Sol-Gel Carrier Systems for Controlled Drug Delivery. *J. Sol-Gel Sci. Technol.* **1998**, *13*, 277–281.
21. Galarneau, A.; Nader, A.; Guenneau, F.; Di Renzo, F.; Gedeon, A. Understanding the Stability in Water of Mesoporous SBA-15 and MCM-41. *J. Phys. Chem. C* **2007**, *111*, 8268–8277.
22. Andersson, J.; Rosenholm, J.; Areva, S.; Lindén, M. Influences of Materials Characteristics on Ibuprofen Drug Loading and Release Profiles from Ordered Micro- and Mesoporous Silica Matrices. *Chem. Mater.* **2004**, *16*, 4160–4167.
23. Rosenholm, J. M.; Lindén, M. Towards Establishing Structure-Activity Relationships for Mesoporous Silica in Drug Delivery Applications. *J. Controlled Release* **2008**, *128*, 157–164.
24. Rosenholm, J. Modular Design of Mesoporous Silica Materials: Towards Multifunctional Drug Delivery Systems. Thesis. D.Sc.(Tech.). Department of Physical Chemistry, Faculty of Technology, Abo Akademi University, 2008..
25. Hartmann, M. Ordered Mesoporous Materials for Bioadsorption and Biocatalysis. *Chem. Mater.* **2005**, *17*, 4577–4593.
26. Vallet-Regí, M.; Balas, F.; Arcos, D. Mesoporous Materials for Drug Delivery. *Angew. Chem., Int. Ed.* **2007**, *46*, 7548–7558.
27. Trewyn, B. G.; Giri, S.; Slowing, I. I.; Lin, V. S.-Y. Mesoporous Silica Nanoparticle Based Controlled Drug Release, Drug Delivery, and Biosensor Systems. *Chem. Commun.* **2007**, 3236–3245.
28. Giri, S.; Trewyn, B. G.; Lin, V. S.-Y. Mesoporous Silica Nanomaterial-Based Biotechnological and Biomedical Delivery Systems. *Nanomedicine* **2007**, *2*, 99–111.
29. Slowing, I. I.; Trewyn, B. G.; Giri, S.; Lin, V. S.-Y. Mesoporous Silica Nanoparticles for Drug Delivery and Biosensing Applications. *Adv. Funct. Mater.* **2007**, *17*, 1225–1236.
30. Slowing, I. I.; Vivero-Escoto, L.; Wu, C.-W.; Lin, V. S.-Y. Mesoporous Silica Nanoparticles as Controlled Release Drug Delivery and Gene Transfection Carriers. *Adv. Drug Delivery Rev.* **2008**, *60*, 1278–1288.
31. Lu, J.; Liong, M.; Zink, J. I.; Tamanoi, F. Mesoporous Silica Nanoparticles as a Delivery System for Hydrophobic Anticancer Drugs. *Small* **2007**, *3*, 1341–1346.
32. Liong, M.; Lu, J.; Kovochich, M.; Xia, T.; Ruhem, S. G.; Nel, A. E.; Tamanoi, F.; Zink, J. I. Multifunctional Inorganic Nanoparticles for Imaging, Targeting, and Drug Delivery. *ACS Nano* **2008**, *2*, 889–896.
33. Slowing, I. I.; Trewyn, B. G.; Lin, V. S.-Y. Mesoporous Silica Nanoparticles for Intracellular Delivery of Membrane-Impermeable Proteins. *J. Am. Chem. Soc.* **2007**, *129*, 8845–8849.
34. Rosenholm, J. M.; Penninkangas, A.; Lindén, M. Amino-Functionalization of Large-Pore Mesoscopically Ordered Silica by a One-Step Hyperbranching Polymerization of a Surface-Grown Polyethyleneimine. *Chem. Commun.* **2006**, *37*, 3909–3911.
35. Rosenholm, J. M.; Lindén, M. Wet-Chemical Analysis of Surface Concentration of Accessible Groups on Different Amino-Functionalized Mesoporous SBA-15 Silicas. *Chem. Mater.* **2007**, *19*, 5023–5034.
36. Barbé, C.; Bartlett, J.; Kong, L.; Finnie, K.; Lin, H. Q.; Larkin, M.; Calleja, S.; Bush, A.; Calleja, G. Silica Particles: A Novel Drug Delivery System. *Adv. Mater.* **2004**, *16*, 1959–1966.
37. Rosenholm, J. M.; Duchanoy, A.; Lindén, M. Hyperbranching Surface Polymerization as a Tool for Preferential Functionalization of the Outer Surface of Mesoporous Silica. *Chem. Mater.* **2008**, *20*, 1126–1133.
38. Fuller, J. E.; Zugates, G. T.; Ferreira, L. S.; Ow, H. S.; Nguyen, N. N.; Wiesner, U. B.; Langer, R. S. Intracellular Delivery of Core-Shell Fluorescent Silica Nanoparticles. *Biomaterials* **2008**, *29*, 1526–1532.
39. Slowing, I. I.; Trewyn, B. G.; Lin, V.S.-Y. Effect of Surface Functionalization of MCM-41-Type Mesoporous Silica Nanoparticles on the Endocytosis by Human Cancer Cells. *J. Am. Chem. Soc.* **2006**, *128*, 14792–14793.
40. Yu, K. O.; Grabinski, C. M.; Schrand, A. M.; Murdock, R. C.; Wang, W.; Gu, B.; Schlager, J. J.; Hussain, S. M. Toxicity of Amorphous Silica Nanoparticles in Mouse Keratinocytes. J. Nanopart. Res. DOI 10.1007/s11051-008-9417-9.
41. Chan, S. Y.; Empig, C. J.; Welte, F. J.; Speck, R. F.; Schmaljohn, A.; Kreisberg, J. F.; Goldsmith, M. A. Folate Receptor-a is a Cofactor for Cellular Entry by Marburg and Ebola Viruses. *Cell* **2001**, *106*, 117–126.
42. Vallhov, H.; Gabrielsson, S.; Strømme, M.; Schydenius, A.; Garcia-Bennett, A. E. Mesoporous Silica Particles Induce Size Dependent Effects on Human Dendritic Cells. *Nano Lett.* **2007**, *7*, 3576–3582.
43. Chung, T.-H.; Wu, S.-H.; Yao, M.; Lu, C.-W.; Lin, Y.-S.; Hung, Y.; Mou, C.-Y.; Chen, Y.-C.; Huang, D.-M. The Effect of Surface Charge on the Uptake and Biological Function of Mesoporous Silica Nanoparticles in 3T3-L1 Cells and Human Mesenchymal Stem Cells. *Biomaterials* **2007**, *28*, 2959–2966.
44. Pasqua, A. J.; Sharma, K. K.; Shi, Y.-L.; Toms, B. B.; Oullette, W.; Dabrowiak, J. C.; Asefa, T. Cytotoxicity of Mesoporous Silica Nanomaterials. *J. Inorg. Biochem.* **2008**, *102*, 1416–1423.
45. Lu, F.; Hung, Y.; Mou, C.-Y. Size Control of Well-Dispersed, Uniformed Mesoporous Silica Nanoparticles and the Size Effect on Cell Labeling. *6th International Mesostructured Materials Symposium Book of Abstracts*; Presses Universitaires de Namur: Belgium, The Netherlands, 2008; p R-015.
46. Lison, D.; Thomassen, L. C. J.; Rabolli, V.; Gonzalez, L.; Napierska, D.; Seo, J. W.; Kirsch-Volders, M.; Hoet, P.; Kirschhock, C. E. A.; Martens, J. A. Nominal and Effective Dosimetry of Silica Nanoparticles in Cytotoxicity Assays. *Toxicol. Sci.* **2008**, *104*, 155–162.
47. Mrsny, R. J. Active Targeting Strategies in Cancer with a Focus on Potential Nanotechnology Applications. In *Nanotechnology for Cancer Therapy;* Amiji, M. M., Ed.; CRC Press: Boca Raton, FL, 2007; pp 19−42.
48. Saul, J. M.; Annapragada, A. V.; Bellamkonda, R. V. A Dual-Ligand Approach for Enhancing Targeting Selectivity of Therapeutic Nanocarriers. *J. Controlled Release* **2006**, *114*, 277–287.
49. Nakamura, T.; Yamada, Y.; Yano, K. Direct Synthesis of Monodispersed Thiol-Functionalized Nanoporous Silica Spheres and Their Application to a Colloidal Crystal Embedded with Gold Nanoparticles. *J. Mater. Chem.* **2007**, *17*, 3726–3732.
50. Möller, K.; Kobler, J.; Bein, T. Colloidal Suspensions of Nanometer-Sized Mesoporous Silica. *Adv. Funct. Mater.* **2007**, *17*, 605–612.